July 2006

Influence of Non-Stoichiometry on the Structure and Properties of $Ba(Zn_{1/3}Nb_{2/3})O_3$ Microwave Dielectrics. IV. Tuning τ_f and the Part Size Dependence of $Q \times f$

Hui Wu
University of Pennsylvania

Peter K. Davies
University of Pennsylvania, davies@lrsm.upenn.edu

Copyright The American Ceramic Society. Reprinted from *Journal of the American Ceramic Society*, Volume 89, Issue 7, July 2006, pages 2271-2278.

Influence of Non-Stoichiometry on the Structure and Properties of $Ba(Zn_{1/3}Nb_{2/3})O_3$ Microwave Dielectrics. IV. Tuning τ_f and the Part Size Dependence of $Q \times f$

Abstract

High Q ceramics of $Ba_3W_2O_9$ (BW)-substituted $Ba(Zn_{1/3}Nb_{2/3})O_3$ (BZN) were prepared with a zero τ_f through the partial substitution of Zn by Ni and Co. The small concentrations of B-site vacancies introduced by the substitution of BW accelerated the kinetics and stability of the cation ordering and lowered the sintering temperature. Dense, zero τz_f, ordered solid solutions such as $0.99Ba(Zn_{0.3}Co_{0.7})_{1/3}Nb_{2/3}O_3$–0.01BW with ε_r=34.4 and $Q \times f$=82 000 at ~8 GHz could be obtained after sintering at 1380°C for 5 h and annealing at 1300°C for 24 h. Partially ordered ceramics in the Zn/Co and Zn/Ni solid solutions show a large gradient in the ordering throughout the pellets, which produces a resonant frequency dependence of their $Q \times f$ value. The ordering gradient is associated with the increased constraints on the growth of the 1:2 ordered structure within the interior of larger and thicker pellets and can be minimized by extended annealing.

journal

J. Am. Ceram. Soc., 89 [7] 2271–2278 (2006)
DOI: 10.1111/j.1551-2916.2006.01010.x

Influence of Non-Stoichiometry on the Structure and Properties of $Ba(Zn_{1/3}Nb_{2/3})O_3$ Microwave Dielectrics. IV. Tuning τ_f and the Part Size Dependence of $Q \times f$

Hui Wu and Peter K. Davies†

Department of Materials Science and Engineering, University of Pennsylvania, Philadelphia, Pennsylvania 19104-6272

High Q ceramics of $Ba_3W_2O_9$ (BW)-substituted $Ba(Zn_{1/3}Nb_{2/3})O_3$ (BZN) were prepared with a zero τ_f through the partial substitution of Zn by Ni and Co. The small concentrations of B-site vacancies introduced by the substitution of BW accelerated the kinetics and stability of the cation ordering and lowered the sintering temperature. Dense, zero τ_f, ordered solid solutions such as $0.99Ba(Zn_{0.3}Co_{0.7})_{1/3}Nb_{2/3}O_3$–0.01BW with $\varepsilon_r = 34.4$ and $Q \times f = 82\,000$ at ~8 GHz could be obtained after sintering at 1380°C for 5 h and annealing at 1300°C for 24 h. Partially ordered ceramics in the Zn/Co and Zn/Ni solid solutions show a large gradient in the ordering throughout the pellets, which produces a resonant frequency dependence of their $Q \times f$ value. The ordering gradient is associated with the increased constraints on the growth of the 1:2 ordered structure within the interior of larger and thicker pellets and can be minimized by extended annealing.

I. Introduction

In a previous paper, the substitution of small concentrations of $Ba_3W_2O_9$ (BW) were shown to accelerate the kinetics of cation ordering, increase the stability of the order, and improve the sintering of $Ba(Zn_{1/3}Nb_{2/3})O_3$ (BZN).[1] As a result, BZN–BW ceramics show some of the highest $Q \times f$ values ($Q \times f \sim 118\,500$) reported for a niobate perovskite and approach those of their "super Q" tantalate counterparts. The improvements in the order and properties were associated with the introduction of B-site vacancies that compensate the substitution of BW. It was shown that vacancy-containing BZN perovskites could also be formed over a narrow range of composition in the BaO–ZnO–Nb_2O_5 ternary system.[2] Although the non-stoichiometry is very limited (typically <1% or less), it again has a very large effect on the extent and stability of the B-site order and the sintering, and enables the formation of high Q ceramics with $Q \times f = 110\,000$. While both of these studies focused on optimizing the structure and dielectric losses, all of the BZN ceramics had a non-zero value of the temperature coefficient of resonant frequency ($\tau_f = 20$–25 ppm/°C). This paper focuses on the formation of high Q BW-substituted ceramics with a zero τ_f through the partial substitution of Zn by Ni and Co. During the study, partially ordered ceramics were found to contain a gradient in the ordering from the surface to interior and their $Q \times f$ values were dependent upon the part size and resonant frequency. The lowering of $Q \times f$ with frequency is well known to occur in super Q tantalate ceramics such as BZT and has limited their use for 2 GHz base-station applications. For the Ni- and Co-substituted BZN–BW systems studied in this paper, when the gradient in the order was removed, the dependence of $Q \times f$ on frequency was almost eliminated. Based on this finding, new methodologies are proposed to limit the degradation of $Q \times f$ in large ceramic pucks.

The tuning of the temperature coefficient of resonant frequency (τ_f) of BZN to a zero value has been explored in systems with a variety of different chemistries. For example, the partial replacement of Ba by Sr in solid solutions of $(1-x)BaZn_{1/3}Nb_{2/3}O_3$–$xSr(Zn_{1/3}Nb_{2/3})O_3$ results in a zero τ_f at $x = 0.7$,[3–6] although the $Q \times f$ value is greatly reduced. The lowering of τ_f has also been studied in the $(1-x)$BZN–$(x)Ba(Ni_{1/3}Nb_{2/3})O_3$ (BNN) and $(1-x)$BZN–$(x)Ba(Co_{1/3}Nb)_{2/3}O_3$ (BCoN) systems.[7–12] BCoN undergoes a transformation from a 1:2 ordered to disordered structure at ~1425°C,[13] slightly higher than pure BZN (~1375°C). Therefore, ordered solid solution phases are typically formed in BZN–BCoN after prolonged annealing at 1300°–1400°C; although there is disagreement on the zero-τ_f composition with values ranging from $x = 0.4$ to 0.7 being reported.[7–11] For $Ba(Ni_{1/3}Nb)_{2/3}O_3$, the literature contains contradictory reports for the disordering temperature, which vary from 1400° to >1500°C.[14–17] The X-ray diffraction (XRD) patterns of this phase often contain secondary impurity phases perhaps associated with partial melting and/or volatilization of NiO at high temperature.[14,15,18] Solid solutions of BZN and BNN prepared by the standard mixed oxide method are disordered; ordered phases were obtained using wet chemical methods and the processing dependency of the ordering was suggested to arise from chemical heterogeneities in the samples prepared by conventional techniques.[12] For $(1-x)$BZN–(x)BNN, a zero τ_f composition was identified at $x = 0.7$ where a dense ceramic sintered at 1500°C had $Q \sim 5700$ at 10 GHz.[12]

Compared with the pure Zn-containing BZN or BZT systems, for Ni- or Co-containing perovskites such as BNN, $BaNi_{1/3}Ta_{2/3}O_3$ (BNT), BCoN, and their BZN–BNN and BZN–BCoN solid solutions, the kinetics of cation ordering are considerably slower. Consequently, a very slow-cooling process (e.g., 2°C/h),[8,11,13] long-term sintering (>20 h),[7,10] or prolonged low-temperature annealing (e.g., >50 h),[16,17] is required to maximize the $Q \times f$ value. The enhancement in $Q \times f$ coincides with an improvement in the cation order.[7–11,13,16]

To accelerate the kinetics of the cation ordering, we focused on preparing zero τ_f ceramics in the BW-substituted BZN–BNN and BZN–BCoN systems. The B-site vacancies introduced by the substitution of BW were previously found to be very effective in permitting the formation of well-ordered, high c/a, high Q ceramics of pure BZN.[1] While similar enhancements were found for the Zn/Ni Zn/Co systems, for shorter anneal times, the kinetically limited diffusion of Ni and Co produced a gradient in the ordering throughout the dense pellets. The gradient was found to be responsible for a dependence of their $Q \times f$ on the size and the resonant frequency of the ceramic.

II. Experimental Procedure

Samples in the $(1-y)[(1-x)Ba_3(ZnNb_2)O_9$–$xBa_3(NiNb_2)O_9]$–$yBa_3W_2O_9$ and $(1-y)[(1-x)\ Ba_3(ZnNb_2)O_9$–$xBa_3(CoNb_2)O_9]$–$y$

T. Vanderah—contributing editor

Manuscript No. 21122. Received November 4, 2005; approved February 8, 2006.
This work was financially supported by the National Science Foundation through award DMR 02-13489 and made use of the MRSEC shared experimental facilities supported by the National Science Foundation through award DMR 05-20020.
†Author to whom correspondence should be addressed. e-mail: davies@seas.upenn.edu

$Ba_3W_2O_9$ systems were prepared by standard solid-state methods. The concentration of BW was fixed at $y = 0.01$. Stoichiometric amounts of $BaCO_3$ (Cerac, 99.9%), Nb_2O_5 (Cerac, 99.95%), ZnO (Cerac, 99.95%), NiO (Cerac, 99.95%), CoO (Cerac, 99.95%), and WO_3 (Cerac, 99.5%) were mixed and calcined at 1000°C to expel CO_2. The products were then ball milled in ethanol with Y-stabilized zirconia media and annealed at 1100°–1200°C for 10 h with an intermediate ball milling for 4 h to obtain single-phase powders. After a second ball mill for 6 h, the samples were dried and pressed isostatically into pellets at 80 000 psi. The pellets were buried in sacrificial powders of the same composition on a piece of platinum (Pt) foil. The Pt foil tray with the pellets and their muffling powders was placed in an alumina crucible together with a small amount of additional ZnO and NiO/CoO powder; the crucible was covered with a flat lid. The effectiveness of this method in maintaining the initial stoichiometry of the pellets was monitored through the weight of the ceramics after each heat treatment; no gains or loss in weight were observed. BZN–BW–BNN could be sintered to a high density (>94%) at 1420°–1440°C and BZN–BW–BCoN at 1380°–1400°C. The subsequent low-temperature annealing was conducted at 1300°C for various times (6–48 h) to monitor the improvement in the ordering and the dielectric properties.

XRD patterns were collected with a Rigaku diffractometer (The Woodlands, TX) using a Cu$K\alpha$ source operated at 45 kV and 30 mA. Equilibration of the samples was gauged by the absence of any changes in the relative intensities of the weak superlattice peaks associated with the cation ordering and splitting of any reflections in the XRD patterns after additional heat treatment. The unit cell parameters were refined by a least-squares procedure using data collected over the range of 10°–140° 2θ with a slow scan speed (0.2°/min) and a step size of 0.02°. Scanning electron microscopy (SEM) study was performed on the thermally etched ceramic samples using a JEOL 6300F FEG HRSEM (Peabody, MA) operated at 10 kV.

The relative permittivity, ε_r, was measured from 100 Hz to 1 MHz using the parallel-plate method combined with an HP 4284 A precision LCR meter (Global Test Supply, Wilmington, NC) and a Delta 9920 environment chamber from −150° to 200°C. Measurements of the dielectric loss, $Q = 1/\tan\delta$, and the temperature coefficient of resonant frequency, τ_f, at microwave frequencies were performed using cavity methods with an Agilent HP8720ES network analyzer (Agilent Technologies, Inc., Palo Alto, CA). The temperature coefficient of the resonant frequency (τ_f) was calculated from data collected in the temperature range of 25°–75°C according to $\tau_f = \Delta f \times f_0 \Delta T$, where f_0 is the reference frequency at 25°C.

III. Results

(1) BZN–BNN–$BaW_{2/3}O_3$(BW) System

In a previous study of BZN, low-level (≤ 2 mole %) substitutions of BW accelerated the kinetics of the cation ordering and reduced the sintering temperatures to enable the formation of well-ordered, high c/a, high $Q \times f$ ceramics after a short anneal (12 h) at 1300°C. For this investigation of BZN–BNN solid solutions, the concentration of BW was fixed at 1 mole%, the ratio of Zn:Ni was varied from $x = 0$ to 1, and the compositions were formulated as $0.99[(1-x)BZN–(x)BNN]–0.01[BaW_{2/3}O_3]$. In all of the heat treatments, appropriate (see Section II) protective environments were used to avoid any gain or loss of the components. Figure 1 shows XRD patterns of samples with $x = 0$, 0.5, 0.7, and 1.0, which were sintered between 1420° and 1440°C and then annealed at 1300°C for 24 h. Single-phase perovskites were formed throughout the entire range of solid solution and, in contrast to a previous report,[12] contained additional reflections associated with the formation of a 1:2 B-site ordered structure.

Compared with BZN–BW ($x = 0$), where the highest degree of order was achieved after 12 h of annealing at 1300°C, the kinetics of the ordering in the BZN–BNN–BW solid solutions

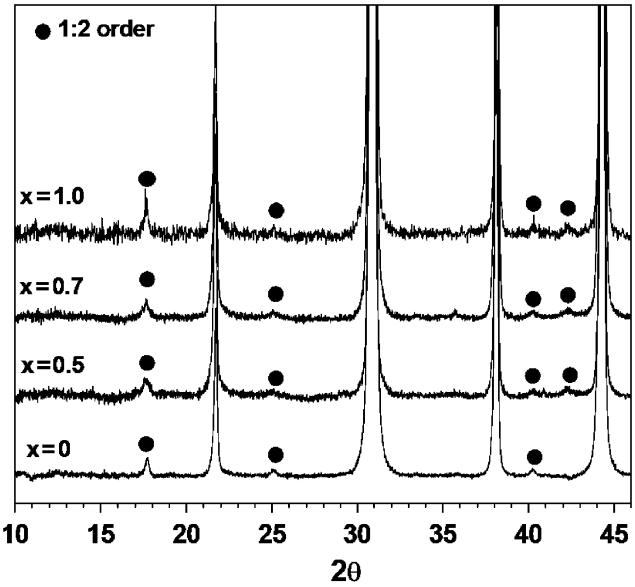

Fig. 1. X-ray diffraction patterns of $0.99[(1-x)Ba(Zn_{1/3}Nb_{2/3})O_3–(x)Ba(Ni_{1/3}Nb_{2/3})O_3(BNN)] -0.01[BaW_{2/3}O_3]$ with $x = 0$, 0.5, 0.7, and 1.0 after annealing at 1300°C for 24 h.

were slow and at least 20 h of annealing were srequired for the intensity of the $(100)_{order}$ superlattice reflection to reach their maximum value. The slower kinetics in the Ni-containing solid solutions also resulted in a range of non-equilibrium states where the extent of the order varies throughout the depth of the ceramic samples. By slicing the pellets to different depths after each heat cycle, the evolution of the variation in the order was examined from the surface to the interior of the dense pellet. To avoid any preferred orientation, the pellet slices were crushed before characterization by XRD. Figure 2 shows the changes observed in the lower angle regions of the XRD patterns throughout a pellet of a sample with $x = 0.7$ (0.99(0.3BZN–0.7BNN) −0.01BW) after sintering at 1430°C for 5 h (Fig. 2(a)), and after a subsequent anneal at 1300°C for 12 h (Fig. 2(b)) and 20 h (Fig. 2(c)), respectively. The XRD patterns of the as-sintered sample contain weak and diffuse superlattice reflections; these become sharper and more intense as the annealing time is increased. In all three samples, the intensity and width (FWHM) of the ordering reflections vary throughout the depth of the pellet. The change in the relative intensity and width of the $(100)_{order}$ reflection, the c/a ratio, and the cell volume throughout each pellet is shown in Fig. 3. While every signature of the order is improved with prolonged annealing, it is evident that the extent of cation order, particularly in the pellets annealed at 1300°C for 12 h, is higher in the near surface region compared with the interior. The large difference between the order at the surface and interior in the 1300°C 12 h annealed ceramic is reduced in the poorly ordered as-sintered samples and also in the samples that approach an equilibrium well-ordered state after annealing at 1300°C for 20 h. The dispersion in the degree of order leads to significant changes in their dielectric response, which are described below.

Similar to the results for pure BZN,[1] the substitution of BW was effective in lowering the sintering temperature of the BZN–BNN ceramics, which reached a high density (>95%) at 1420°–1440°C, approximately 100°C lower than those reported in previous investigations of the system.[12] After sintering at 1430°C for 5 h, thermally etched samples with $x = 0.5$ and 0.7 revealed a well-densified microstructure comprised of large homogenous grains with sizes in the range 5–8 μm; see Figs. 4(a) and (b). The ceramics of BZN–BNN–BW sintered at 1420°–1440°C show no evidence for the involvement of a liquid phase; however, the SEM images collected from samples sintered at a higher temperature (e.g., 1480°C for 4 h) reveal features consistent with liquid phase sintering (Fig. 4(c)), which were also observed in the

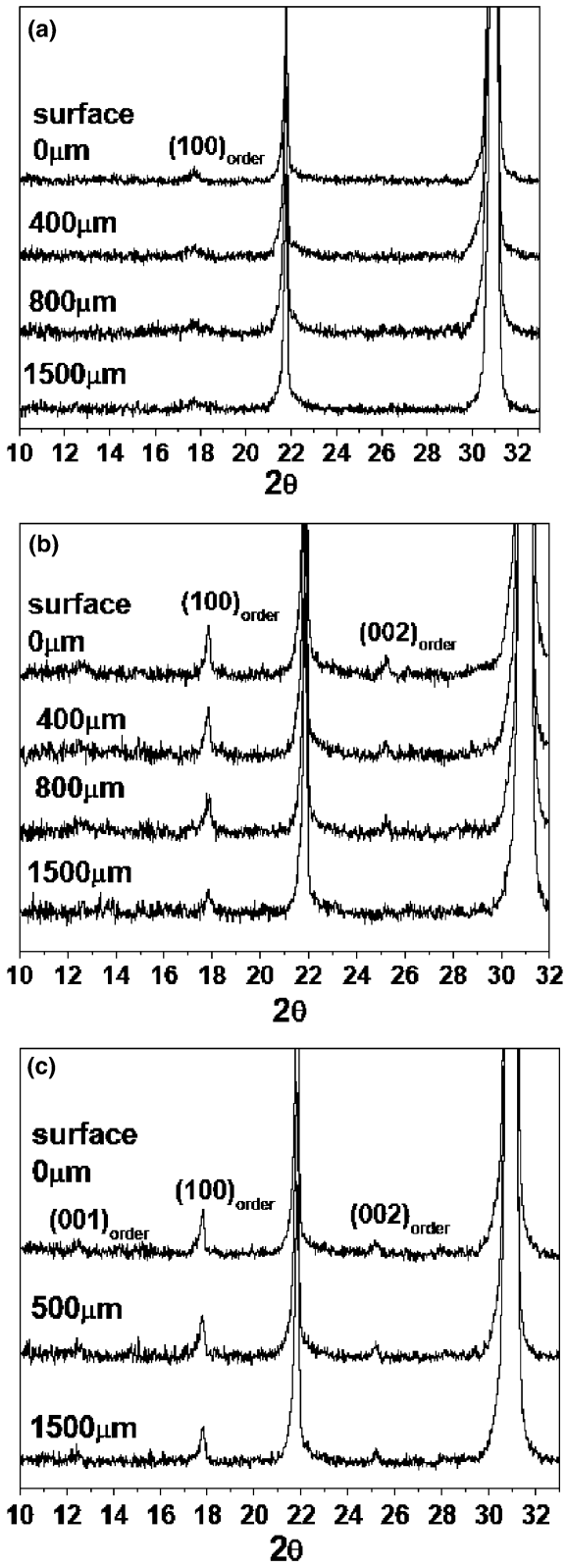

Fig. 2. Lower angle regions of the X-ray patterns of a sectioned pellet sample of 0.99(0.3BZN–0.7BNN)–0.01BW ($x = 0.7$): (a) after sintering at 1430°C for 5 h, and after subsequent anneals at 1300°C for 12 h (b) and 20 h (c). The depth of the sectioned sample is shown for each pattern.

studies of BZN–BW.[1] EDS analysis indicated that the grains and grain boundary compositions are close to their expected stoichiometry with a small enrichment of Ba and W at the grain boundary regions. Apparently, the temperature (~1410°C) of the peritectic reaction identified for BZN–BW[1] is increased by the presence of Ni, which is consistent with data reported for liquid phase formation in pure BNN.[17]

As expected, the substitution of BNN reduces the temperature coefficient of resonant frequency of BZN–BW ($\tau_f = +21$–23 ppm/°C); the variation of τ_f with x is shown in Fig. 5. A $\tau_f = 0$ was obtained for the composition close to $x = 0.7$ (Zn:Ni = 3:7). The τ_f of all the samples annealed at 1300°C for 20 h were slightly lower than those of the as-sintered ceramic. This is probably related to the changes in the cation–anion bond strengths and bond lengths during the ordering process.[19] The $Q \times f$ values and relative dielectric constants (ε) after the 20 h annealing are shown in Fig. 6. To confirm their reproducibility, the data were collected from specimens prepared in identical ways from several different batches of the starting powders. The zero τ_f composition with $x = 0.7$ has a mean $Q \times f = 71\,000$ at 8.2–9.2 GHz, and a dielectric constant = 32.2.

Besides their variation with composition, the dielectric loss properties of BZN–BNN–BW also show an interesting dependence on the sample dimensions. In a standard cavity measurement, the approximate resonant frequency of an isolated dielectric resonator can be estimated from $f_{GHz} = \frac{34}{a\sqrt{\varepsilon_r}}\left[\frac{a}{t} + 3.45\right]$,[20] where a and t are the radius and thickness of the resonator, respectively. For pellets with the same composition and a similar relative density, diameter ($d = 2a \sim 6.8$ mm), and relative dielectric constant (Table I), f is primarily determined by the aspect ratio (t/d or $t/2a$) and should be inversely proportional to t/d. Therefore, it is generally observed that thicker pellets resonate at lower frequencies (see Fig. 7). For impurity-free dielectric resonators, where the losses are primarily because of phonon scattering, the loss typically increases linearly with f and the $Q \times f$ product should be independent of f. In that case, the $Q \times f$ product should be independent of t/d and higher Q's should be observed in thicker pellets where the resonance occurs at a lower frequency. It should be noted that refinements to the above equation are necessary for analysis of Q and f of pellets investigated over a wide range of frequency and aspect ratio, and for ring resonators.[20,21] However, for the range of frequency and aspect ratio of the samples explored in this investigation, the effect of these higher order corrections on the Q's that we observed is less than 0.1%.

$Q \times f$ data for ceramics of BZN–BNN–BW with different aspect ratios are shown in Fig. 7; a reproducible and significant dependence of $Q \times f$ on the aspect ratio, in particular for those samples annealed at 1300°C for 12 h, is clearly evident. The dependence of $Q \times f$ on f for the 1300°C, 12 h pellets is further highlighted by the plot in Fig. 8(a) where the $Q \times f$ product of the $x = 0.5$ and 0.7 samples is seen to increase significantly with frequency, while the data for the corresponding 12 h annealed Zn (Ni-free) ceramic are essentially independent of f over the range investigated. After a prolonged annealing (e.g., 20 h), the $Q \times f$ values of the BZN–BNN–BW increase at all frequencies and reach values 50%–80% higher than the as-sintered samples. The extended annealing also reduces the dependence of $Q \times f$ on the aspect ratio (Fig. 7), which remains almost constant ($Q \times f$ ~80 000 for $x = 0.5$; ~70 000 for $x = 0.7$) over the 7.9–9.5 GHz range. The increase in the Q and $Q \times f$ values is closely related to the increase in the cation order observed for each specimen (Fig. 3). Their dependence on the aspect ratio, and therefore frequency, after a 12 h anneal at 1300°C coincides with the formation of pellets with the largest gradient in the degree of order and ordered domain size (Fig. 3).

(2) BZN–BCoN–BaW$_{2/3}$O$_3$(BW) System

The formation of zero-τ_f compositions was also investigated in the BZN–BCoN–BW system where the concentration of BW was again fixed at 1 mole%. Figure 9 shows the XRD patterns collected from crushed BZN–BCoN–BW pellets annealed at 1300°C for >20 h after sintering at 1380°C for 5 h. The patterns are free of peaks from impurity phases and all the solid solutions form a 1:2 ordered perovskite. Similar to BZN–BNN–BW, after annealing for intermediate times (12 h at 1300°C), the degree of order and domain size vary throughout the thickness of the pellet, with the interior showing a much lower degree of

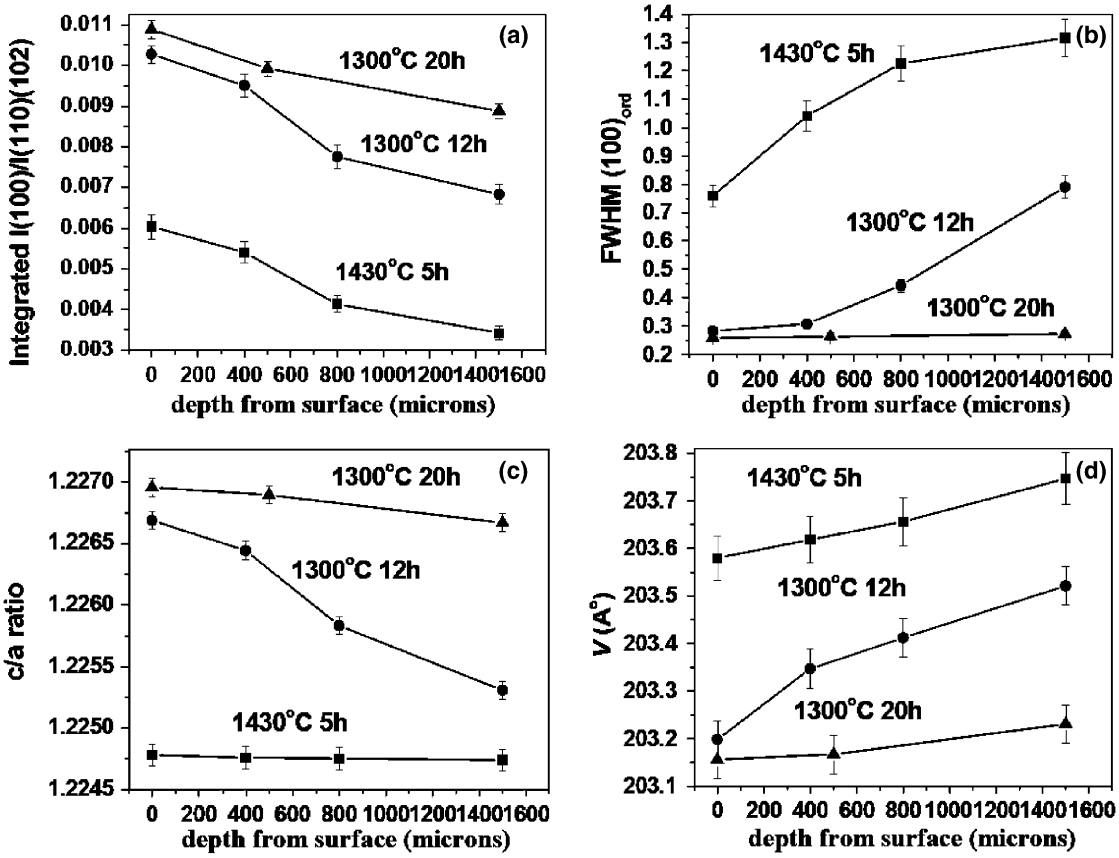

Fig. 3. Variation in the relative intensity (a), and width (b) of the $(100)_{order}$ reflection, the c/a ratio (c), and the cell volume (d), throughout the pellets of 0.99(0.3BZN–0.7BNN)–0.01BW.

order compared with the near surface regions. The XRD patterns and trends in the structural parameters collected from sliced pellets were almost identical to those shown in Fig. 2 for BNN and are not reiterated here.

All of the BZN–BcoN–BW solid solutions could be sintered to a high density (>95%) after a 5 h heat at 1380°C, again, this is lower than the temperatures previously reported for the BW-free system.[7–11] The SEM images (Fig. 10) reveal a dense homogeneous microstructure with a grain size ~5–8 μm. Figure 11 shows the variation of τ_f with composition; a zero τ_f was obtained close to $x = 0.7$ (70% Co–30% Zn). The $Q \times f$'s and relative dielectric constants of the samples after equilibration at 1300°C for >20 h are shown in Fig. 12. The zero-τ_f composition has $Q \times f \sim 82\,000$ at 7.7–8.8 GHz and $\varepsilon = 34.4$. The $Q \times f$ values of the pellets annealed for intermediate times also show an aspect ratio and frequency dependence, which again could be minimized by annealing at a low temperature for a longer time (typically 20 h at 1300°C).

The correlation between the changes in structure and Q is further illustrated by the data in Fig. 13, where the $Q \times f$ of BZN–BCoN–BW and BZN–BNN–BW ceramics was monitored as a function of the extent of annealing at 1300°C. In each case, $Q \times f$ increases systematically with the annealing time, consistent with the associated increase in the degree of ordering (Fig. 3). The changes in $Q \times f$ reported in Endo *et al.*[7] for even longer heat treatments of BW-free BZN–BCoN are also plotted in Fig. 13. The rate of increase in Q, which reflects the rate of increase in the ordering, is greater in the BW-containing solid solutions that reach a higher degree of order and higher Q after a shorter annealing time.

IV. Discussion

High Q compositions with a zero τ_f were identified in the BZN–BNN–BW and BZN–BCoN–BW solid solution systems. Consistent with the results obtained in previous work on pure BZN, BW was found to be an effective additive in accelerating the ordering kinetics and promoting the formation of a well 1:2 ordered structure with a high c/a distortion and a high Q in the BZN–BNN and BZN–BCoN systems. We believe that the enhancement in the order and the accelerated kinetics are related to the small concentrations of B-site vacancies introduced by BW and the formation of ordered structures with $Ba[(Zn_{1-x}Co/Ni_x)_{0.99}Vac_{0.01}]_{1/3}(Nb_{0.99}W_{0.01})_{2/3}O_3$); these and the resultant changes in the local stability of the anions were identified and discussed previously for the BZN–BW system.[1] Rather than reiterate these arguments here, in this paper we focus on new features of the ordering discovered in the BZN–BNN–BW and BZN–BCoN–BW systems that lead to gradients in the degree of order in partially annealed dense pellets and produce an aspect ratio and frequency dependence of their $Q \times f$ values.

In BW-substituted BZN, no obvious ordering gradient or aspect ratio dependence of the $Q \times f$ is observed in either the as-sintered (1390°C, 5 h) or annealed (1300°C for 12 h) samples. The small concentrations of Zn vacancies introduced by BW are effective in removing any significant kinetic barriers to the formation of well-ordered ceramics, which form a homogenous structure comprised of large ordered domains with a high c/a and Q after a short anneal. The formation of ceramics with a gradient in the ordering in the dense pellets of BZN–BNN–BW and BZN–BCoN–BW is presumably related to a lower diffusivity of the Ni and Co cations compared with Zn. The increased kinetic limitations on the ordering process in the Ni- and Co-containing systems are consistent with the observations made on other perovskites such as $Ba_3NiNb_2O_9$ (BNN), $Ba_3NiTa_2O_9$ (BNT), BCoN, and their various solid solutions, which, compared with their Zn counterparts, require much slower cooling rates,[8,11,13] longer sintering[7,10] or longer low-temperature annealing[16, 17] to reach a high degree of order and a maximum Q. The large gradients in the degree of order and ordered domain size (Fig. 3) and the associated dependence of the $Q \times f$ on as-

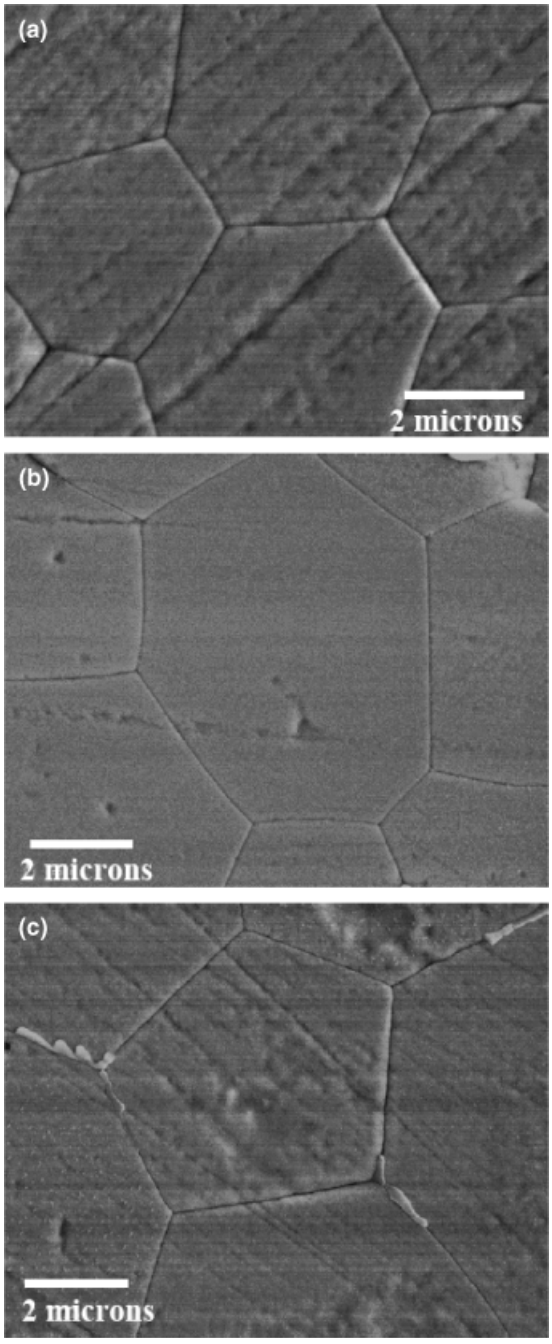

Fig. 4. Scanning electron microscopic images of thermally etched BZN–BNN–BW with (a) $x = 0.5$ (1430°C, 5 h sintering) and (b) $x = 0.7$ (1480°C 4 h sintering).

pect ratio (Fig. 7) were only observed in dense pellets of BZN–BNN–BW and BZN–BCoN–BW with non-equilibrium, "intermediate" or "partial" order. The ordering gradient and aspect ratio dependence is present, but much smaller, in the poorly ordered as-sintered samples and is greatly reduced by prolonged annealing (20 h at 1300°C), although even in the longer annealed ceramics the ordered domain size and c/a ratio in the interior of the pellet did not reach the value observed at the surface.

In the study of BZN–BW,[1] it was noted that the continuous expansion of the 1:2 ordered structure along c and the associated rhombohedral distortion of the parent cubic sub-cell introduce a "ferroelastic-type" strain, which was suggested to constrain the domain growth along the c direction. Support for that model was provided by the large difference in the magnitude of the c/a lattice distortion observed in dense pellets and free powders of BZN.[1] Similarly, in the ordered pellets of BZN–BNN–BW and BZN–BCoN–BW, the constraints on the domain growth and

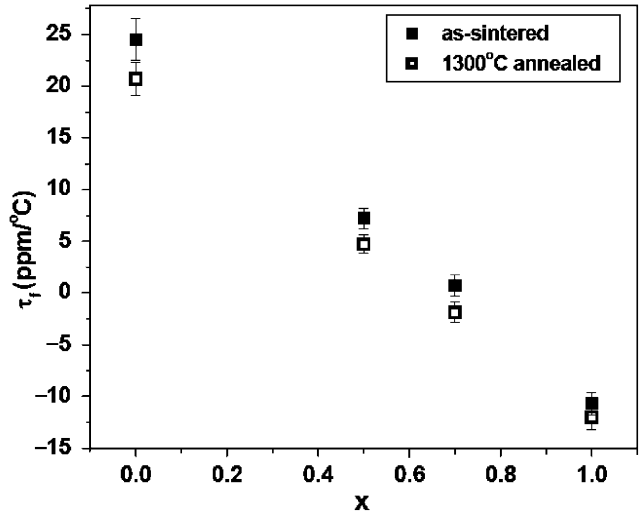

Fig. 5. Variation of τ_f with composition in $0.99[(1-x)BZN–(x)BNN]–(0.01)BW$.

lattice distortion will be different at the free surface and interior of the pellet. The large constraints in the interior are reflected by the lower degree of order, smaller domain size, and lower c/a of the 12 h annealed ceramics, which only approach those of the surface regions after a more extended annealing.

For ferroelastic systems,[22] the formation of larger domains at the surface of a dense ceramic was shown to arise from the relaxation of the domain boundaries at a free surface. For our systems, thicker pellets with a lower surface to volume ratio show a larger ordering gradient and contain a higher volume percentage of a "constrained" ordered phase; we propose that this is the major factor in mediating their dielectric loss. As the aspect ratio is decreased, the thinner pellets have a smaller domain gradient, contain a lower volume percent of the constrained domains, and therefore have a higher $Q \times f$. The change in the volume fraction of the constrained phase in turn is responsible for the dependence of $Q \times f$ on the aspect ratio and frequency. When the "coring" effect is reduced and ordering becomes homogeneous throughout the pellet, the $Q \times f$ increases and its dependence on frequency is removed.

The different degrees of constraint near the surface and in the interior of the pellets may explain our prior observation of a small gradient in the ordering in dense ceramics of pure BZN[23] where the kinetics are limited by the slower diffusion of Zn in the BW-free stoichiometric system. It is possible that these types of constraint effects are also responsible for intra-grain domain gradients or "core-shell" structures that have been reported for 1:2 other ordered systems.[24–27]

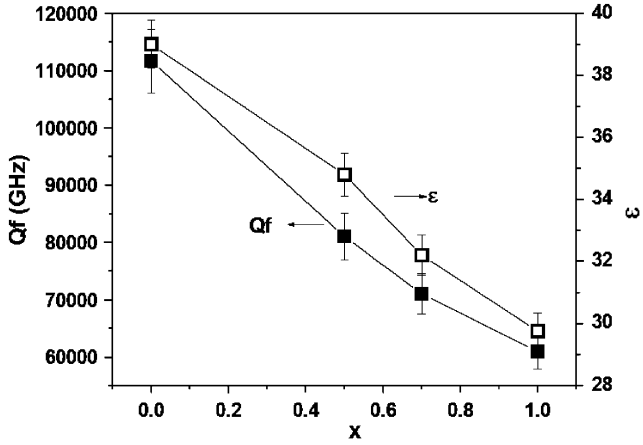

Fig. 6. $Q \times f$ and ε data of $(1-x)BZN–(x)BNN–BW$ after annealing at 1300°C for 20 h.

Table I. Dielectric Properties of BZN–BNN–BW with Different Aspect Ratios After Annealing at 1300°C for 12 h

Zn:Ni	Aspect ratio (t/d)	Density (%)	Dielectric constant (ε_r) at 1M	f_0 (GHz)	Q (at f_0)	τ_f (ppm/°C)
3:7	0.59	96.3	33.9	7.78	6645	0
	0.44	96.7	33.7	8.30	6964	−0.33
	0.25	96.1	33.7	9.70	7761	−0.87
1:1	0.51	96.4	36.3	7.77	7990	+7.28
	0.42	97	36.1	8.20	8598	+6.77
	0.30	96.3	35.8	8.57	8706	+5.68

Although the coring effects and associated $Q \times f$ dependence observed in the Ni/Co systems after a 12 h anneal were absent in similar-sized ceramics of BZN–BW annealed at the same temperature for the same time, it is possible, perhaps likely, that coring effects will be present in the faster-diffusing Zn systems after a shorter anneal time or in larger "puck-sized" ceramics where the constraints on the growth are even larger. For many years, it has been recognized that the $Q \times f$ factors of large pucks of "super Q" microwave perovskites such as $Ba(Zn_{1/3}Ta_{2/3})O_3$ (BZT) prepared for 2 GHz applications are inferior to those of smaller ceramic pieces, where $Q \times f$'s $\geq$ 150 000 have been reported at frequencies close to 10 GHz. Indeed, the specifications of many BZT-based commercial ceramics are only quoted for a 10 GHz resonance, even though their main potential lies in 2 GHz base station applications. The deterioration in $Q \times f$ has often been thought to arise from variations in the degree of volatilization of ZnO in the different-sized parts or to other difficulties associated with the processing of large ceramic parts. We suggest that the reduction in $Q \times f$ at lower frequency is directly related to an increase in the coring of the order and a reduction in the volume percent of a well-ordered phase from the increased constraints on the growth of the 1:2 ordered structure within the interior of the large ceramic pucks. It is possible that this effect could be alleviated through very long anneal times; we propose that a more effective route would be to use chemistries where B-site vacancies are deliberately introduced

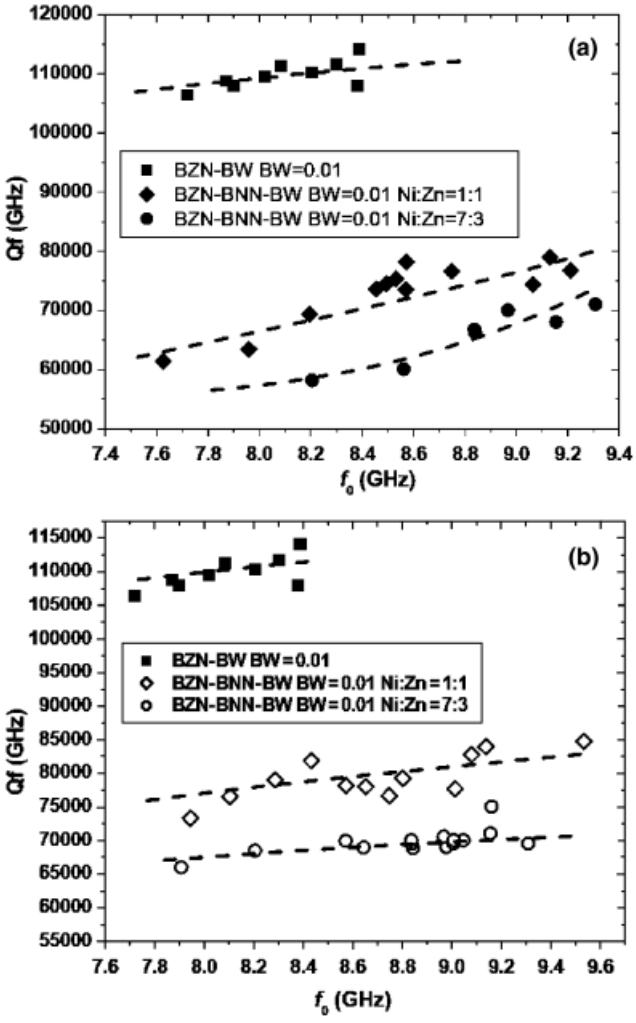

Fig. 8. Resonant frequency dependence of $Q \times f$ for BZN–BW and BZN–BNN–BW ceramics annealed at 1300°C for (a) 12 h and (b) 20 h.

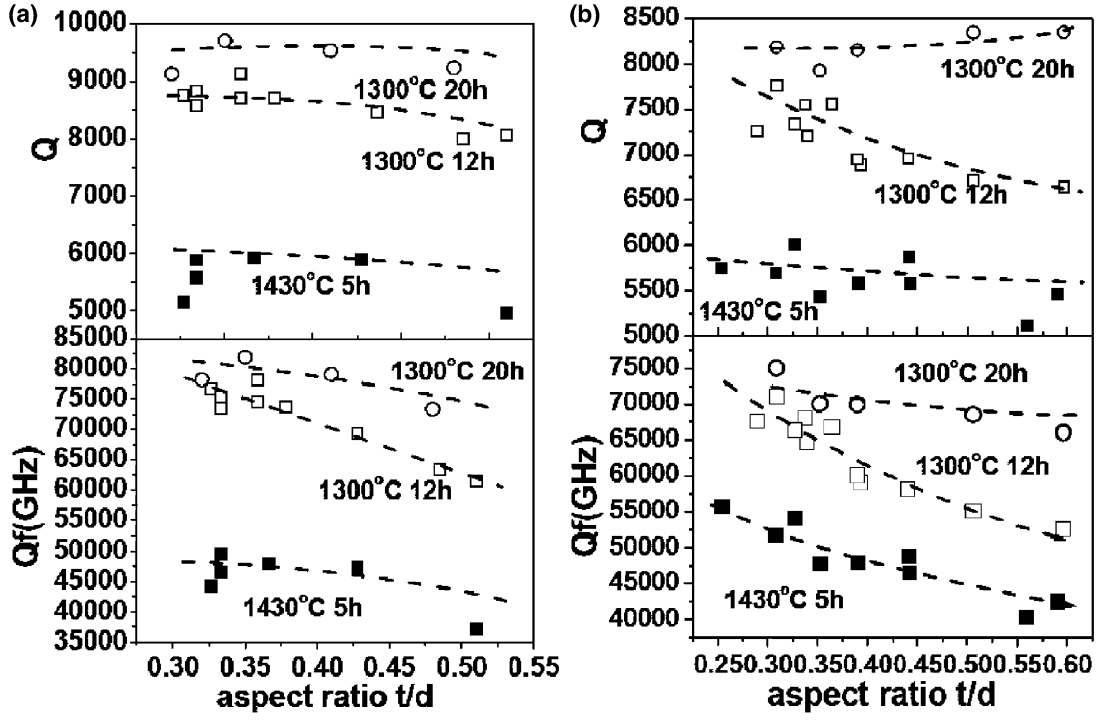

Fig. 7. Variation of $Q \times f$ with aspect ratio (t/d) for sintered and annealed samples of $(1-x)$BZN–(x)BNN–BW with (a) $x = 0.5$ and (b) $x = 0.7$.

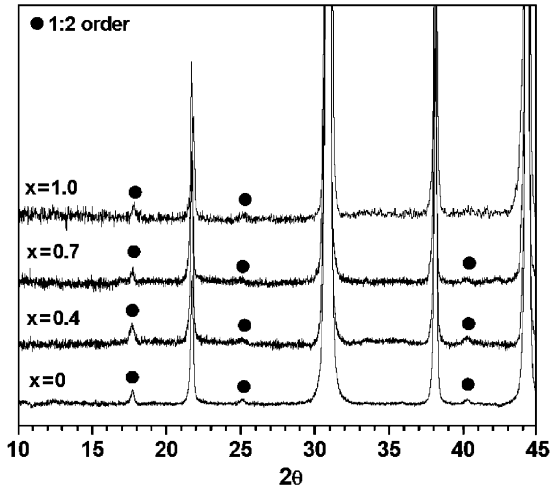

Fig. 9. X-ray diffraction patterns of $0.99[(1-x)Ba(Zn_{1/3}Nb_{2/3})O_3$–$(x)Ba(Co_{1/3}Nb_{2/3})O_3] - 0.01[BaW_{2/3}O_3]$ with $x = 0$, 0.4, 0.7, and 1.0 after annealing at 1300°C for $\geq$ 24 h.

into the starting powders, e.g., through the substitutions of BW investigated in this paper or the non-stoichiometric BZN powders described in our prior work, where the ordering kinetics and the stability of the ordered phase are greatly enhanced.

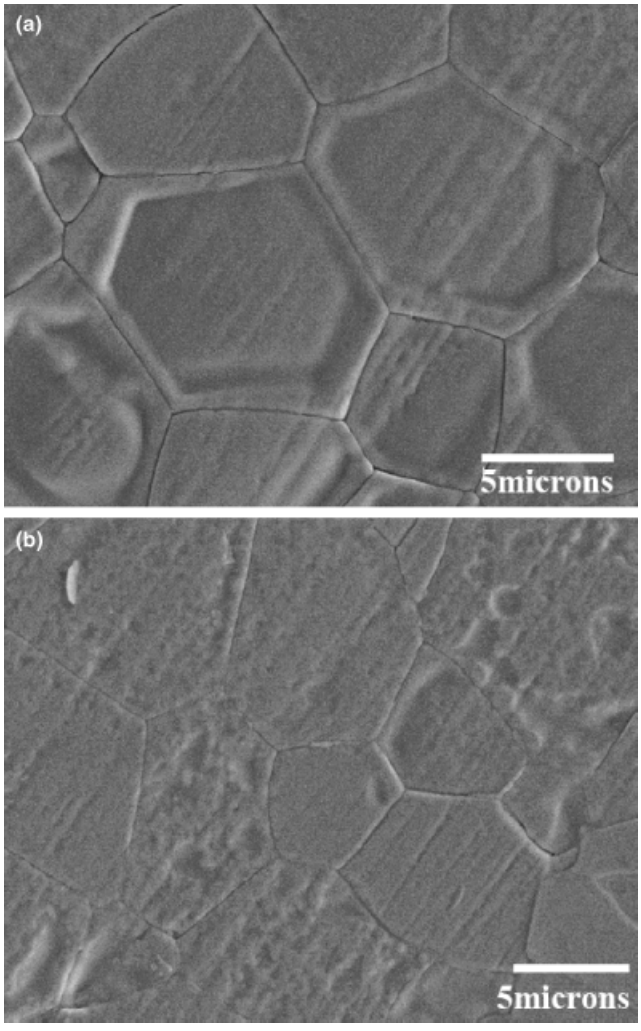

Fig. 10. Scanning electron microscopic images of thermally etched BZN–BCoN–BW with (a) $x = 0.4$ and (b) $x = 0.7$, after sintering at 1380°C for 5 h.

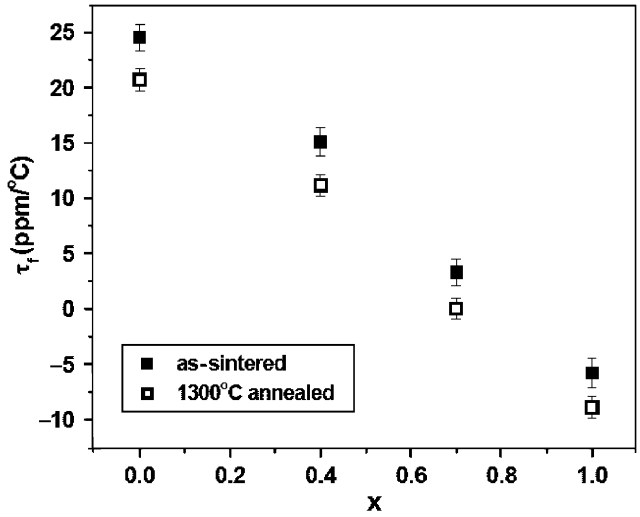

Fig. 11. Variation of τ_f with composition in the $0.99[(1-x)$BZN–(x)BCoN]-(0.01)BW.

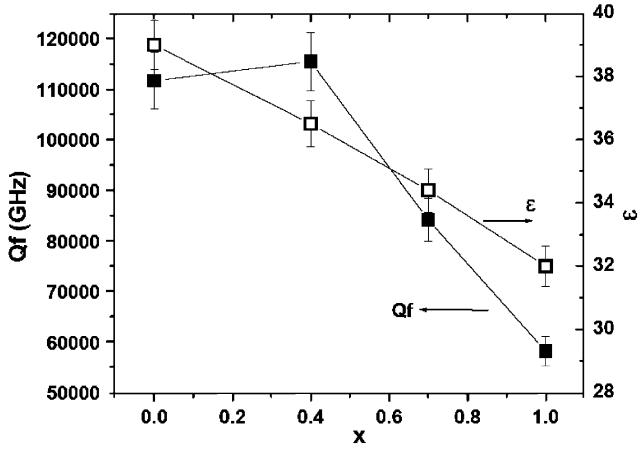

Fig. 12. $Q \times f$ and ε data of BZN–BCoN–BW after annealing at 1300°C for $\geq$ 20 h.

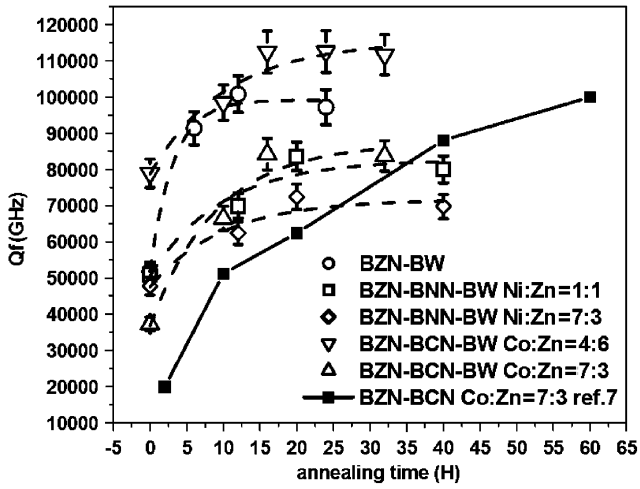

Fig. 13. Change in $Q \times f$ with the time of annealing at 1300°C for BZN–BW, BZN–BNN–BW, BZN–BCoN–BW. Data for BW-free BZN–BCoN were adapted from Endo *et al.*[7]

V. Conclusions

High Q, zero τ_f ceramics were obtained in the $0.99[(1-x)BaZn_{1/3}Nb_{2/3}O_3$–$(x)Ba(Ni/Co_{1/3}Nb_{2/3})O_3]$–$0.01[BaW_{2/3}O_3]$ systems. The zero τ_f was obtained close to $x = 0.7$ in both systems

with $Q \times f$ values of $\sim$71 000 for Zn–Ni and $Q \times f \sim$80 000 for Zn–Co. In agreement with the observations made on pure BZN, BW is effective in accelerating the ordering kinetics and promoting the formation of a well 1:2 ordered structure with a high c/a distortion and a high Q because of the small concentrations of B-site vacancies. Partially ordered dense ceramics show a large gradient in the ordered domain size, which results in an aspect ratio and frequency dependence of their $Q \times f$ values. The reduction in $Q \times f$ at lower frequency is due to an increase in the coring of the order and reduction in the volume percent of a well-ordered phase originating from the increased constraints on the growth of the 1:2 ordered structure within the interior of larger/thicker pellets.

References

[1]H. Wu and P. K. Davies, "Influence of Non-Stoichiometry on the Structure and Properties of $BaZn_{1/3}Nb_{2/3}O_3$ Microwave Dielectrics: I. Substitution of $Ba_3W_2O_9$" *J. Am. Ceram. Soc.*, **89** [7] 2239–49 (2006).

[2]H. Wu and P. K. Davies, "Influence of Non-Stoichiometry on the Structure and Properties of $BaZn_{1/3}Nb_{2/3}O_3$ Microwave Dielectrics: II. Compositional Variations in Pure BZN," *J. Am. Ceram. Soc.*, **89** [7] 2250–63 (2006).

[3]I. M. Reaney, E. L. Colla, and N. Setter, "Dielectric and Structural Characteristics of Ba- and Sr-Based Complex Perovskites as a Function of Tolerance Factor," *Jpn. J. Appl. Phys.*, **33**, 3984–90 (1994).

[4]E. L. Colla, I. M. Reaney, and N. Setter, "Effect of Structural Changes in Complex Perovskites on the Temperature Coefficient of the Relative Permittivity," *J. Appl. Phys.*, **74** [5] 3414–25 (1993).

[5]M. Onoda, J. Kuwata, K. Kaneta, K. Toyama, and S. Nomura, "$Ba(Zn_{1/3}Nb_{2/3})O_3$–$Sr(Zn_{1/3}Nb_{2/3})O_3$ Solid Solution Ceramics with Temperature-Stable High Dielectric Constant and Low Microwave Loss," *Jpn. J. Appl. Phys.*, **21** [12] 1707–10 (1982).

[6]J. S. Kim, J. H. Lee, Y.-S. Lim, J. W. Jang, and I.-T. Kim, "Revisit to the Anomaly in Dielectric Properties of $(Ba_{1-x}Sr_x)(Zn_{1/3}Nb_{2/3})O_3$ Solid Solution Systems," *Jpn. J. Appl. Phys.*, **36**, 5558–61 (1997).

[7]K. Endo, K. Fujimoto, and K. Murakawa, "Dielectric Properties of Ceramics in $Ba(Co_{1/3}Nb_{2/3})O_3$–$Ba(Zn_{1/3}Nb_{2/3})O_3$ Solid Solutions," *J. Am. Ceram. Soc.*, **70** [9] C-215–8 (1987).

[8]R. I. Scott, M. Thomas, and C. Hampson, "Development of Low Cost, High Performance $Ba(Zn_{1/3}Nb_{2/3})O_3$ Based Materials for Microwave Resonator Applications," *J. Eur. Ceram. Soc.*, **23**, 2467–71 (2003).

[9]H. Hughes, D. M. Iddles, and I. M. Reaney, "Niobate-Based Microwave Dielectrics Suitable for Third Generation Mobile Phone Base Stations," *Appl. Phys. Lett.*, **79** [18] 2952–4 (2001).

[10]C.-W. Ahn, H.-J. Jang, S. Nahm, H.-M. Park, and H.-J. Lee, "Effects of Microstructure on the Microwave Dielectric Properties of $Ba(Co_{1/3}Nb_{2/3})O_3$ and $(1-x)$ $Ba(Zn_{1/3}Nb_{2/3})O_3$–(x) $Ba(Co_{1/3}Nb_{2/3})O_3$ Ceramics," *J. Eur. Ceram. Soc.*, **23**, 2473–8 (2003).

[11]D. Muir and D. M. Iddles, "$Ba(Co_{1-x}Zn_x)_{1/3}Nb_{2/3}O_3$ Ceramics for Use as Microwave Dielectric Resonators, in preparation.

[12]S.-Y. Cho, H.-J. Youn, K.-S. Hong, I.-T. Kim, and Y.-H. Kim, "A New Microwave Dielectric Ceramics Based on the Solid Solution System Between $Ba(Ni_{1/3}Nb_{2/3})O_3$ and $Ba(Zn_{1/3}Nb_{2/3})O_3$," *J. Mater. Res.*, **12** [6] 1558–62 (1997).

[13]I. Molodetsky and P. K. Davies, "Effect of $Ba(Y_{1/2}Nb_{1/2})O_3$ and $BaZrO_3$ on the Cation Order and Properties of $Ba(Co_{1/3}Nb_{2/3})O_3$ Microwave Ceramics," *J. Eur. Ceram. Soc.*, **21**, 2587–91 (2001).

[14]T. Kolodiazhnyi, A. Petrica, A. Belous, O. V'yunov, and O. Yanchevskij, "Synthesis and Dielectric Properties of Barium Tantalates and Niobates with Complex Perovskite Structure," *J. Mater. Res.*, **17** [12] 3182–9 (2002).

[15]K. S. Hong, I.-T. Kim, and C.-D. Kim, "Order–Disorder Phase Formation in Complex Perovskite Compounds $Ba(Ni_{1/3}Nb_{2/3})O_3$ and $Ba(Zn_{1/3}Nb_{2/3})O_3$," *J. Am. Ceram. Soc.*, **79** [12] 3218–24 (1996).

[16]I.-T. Kim, Y.-H. Kim, and S. J. Chung, "Ordering and Microwave Dielectric Properties of $Ba(Ni_{1/3}Nb_{2/3})O_3$," *J. Mater. Res.*, **12** [2] 518–25 (1997).

[17]I.-T. Kim, Y.-H. Kim, and S. J. Chung, "Order–Disorder Transition and Microwave Dielectric Properties of $Ba(Ni_{1/3}Nb_{2/3})O_3$ Ceramics," *Jpn. J. Appl. Phys.*, **34**, 4096–103 (1995).

[18]I.-T. Kim, K. S. Hong, and S.-J. Yoon, "Effects of Non-stoichiometry and Chemical Inhomogeneity on the Order–Disorder Phase Formation in the Complex Perovskite Compounds, $Ba(Ni_{1/3}Nb_{2/3})O_3$ and $Ba(Zn_{1/3}Nb_{2/3})O_3$," *J. Mater. Sci.*, **30**, 514–21 (1995).

[19]I. Levin, J. Y. Chan, R. G. Geyer, J. E. Maslar, and T. A. Vanderah, "Cation Ordering Types and Dielectric Properties in the Complex Perovskite $Ca(Ca_{1/3}Nb_{2/3})O_3$," *J. Solid State Chem.*, **156**, 122–34 (2001).

[20]D. Kajfez, "Chapter 1 Introduction"; pp. 1–9 in *Dielectric Resonators*, Edited by D. Kajfez, and P. Guillon. Noble Publishing Corporation, Atlanta, 1998.

[21]R. de Smedt, "Correction Due to a Finite Permittivity for a Ring Resonator in Free Space," *IEEE Trans. Micro. Theo. Tech.*, **MTT-32** 10] 1288–93 (1984).

[22]S. Conti and U. Weikard, "Interaction Between Free Boundaries and Domain Walls in Ferroelastics," *Eur. Phys. J.*, **B41**, 413–20 (2004).

[23]H. Wu and P. K. Davies, "Influence of Non-stoichiometry on the Structure and Properties of $BaZn_{1/3}Nb_{2/3}O_3$ Microwave Dielectrics: III. The Effect of the Muffling Environment," *J. Am. Ceram. Soc.*, **89** [7] 2264–70 (2006).

[24]D. J. Barber, K. M. Moulding, J. Zhou, and M. Li, "Structural Order in $Ba(Zn_{1/3}Ta_{2/3})O_3$, $Ba(Zn_{1/3}Nb_{2/3})O_3$ and $Ba(Mg_{1/3}Ta_{2/3})O_3$ Microwave Dielectric Ceramics," *J. Mater. Sci.*, **32**, 1531–44 (1997).

[25]Y.-W. Kim, J.-H. Park, and J.-G. Park, "Local Cationic Ordering Behavior in $Ba(Mg_{1/3}Nb_{2/3})O_3$ Ceramics," *J. Eur. Ceram. Soc.*, **24**, 1775–9 (2004).

[26]I. M. Reaney, P. L. Wise, I. Qazi, C. A. Miller, T. J. Price, D. S. Cannell, D. M. Iddles, M. J. Rosseinsky, S. M. Moussa, M. Bieringer, L. D. Noailles, and R. M. Ibberson, "Ordering and Quality Factor in $0.95BaZn_{1/3}Ta_{2/3}O_3$–$0.05SrGa_{1/2}Ta_{1/2}O_3$ Production Resonators," *J. Eur. Ceram. Soc.*, **23**, 3021–34 (2003).

[27]I. M. Reaney, I. Qazi, and W. E. Lee, "Order–Disorder Behavior in $Ba(Zn_{1/3}Ta_{2/3})O_3$," *J. Appl. Phys.*, **88** [11] 6708–14 (2000). □